Sensitivity of Projection-Based Near-Far Mitigation Techniques in High-Sensitivity GNSS Software Receivers

Sergi Locubiche-Serra, José A. López-Salcedo, Gonzalo Seco-Granados
Department of Telecommunications and Systems Engineering
Universitat Autònoma de Barcelona (UAB), Spain
Email: sergi.locubiche@uab.cat, jose.salcedo@uab.cat, gonzalo.seco@uab.cat

***Abstract*—One of the difficulties faced by high-sensitivity GNSS receivers is the so-called near-far problem, where the acquisition of weak signals is hampered by the presence of more powerful signals. If countermeasures are not implemented, the presence of near-far may result in loss or false acquisition of weak signals, and consequently the user's position may exhibit a huge error. In this sense, subspace projection techniques become an attractive choice for near-far mitigation purposes due to their effectiveness and low-complexity. However, many questions still remain open to make the techniques implementable in real handheld receivers such as mobile phones, which have not yet been addressed in the literature. This paper contributes with an analysis of the robustness of projection-based mitigation techniques when the synchronization parameters or the data bits of the interferences are not perfectly estimated. On the other hand, the paper also analyses the impact that signal filtering and quantization at the receiver front-end may also have on the near-far mitigation performance. The approaches presented in this paper give an actual idea of what would happen in practice in a real GNSS receiver. To analyse these effects, an extensive simulation campaign was conducted for Galileo E1 signals.**

***Index Terms*—Cross-correlation, GNSS, interference cancellation, near-far mitigation, subspace projection.**

I. Introduction

Global Navigation Satellite Systems (GNSS) are known to be one of the most suitable Location Based Services (LBS)-enabling technologies for a number of reasons [1], [2]: coverage, availability and accuracy in outdoor environments, and maturity of GNSS receiver technology. However, in indoor scenarios or dense-urban canyons (from now on "indoor" environments), where the carrier-to-noise ratio (C/N_0) is typically below 20 dB-Hz [3], GNSS receivers face some limitations such as high attenuation of signals, non-line-of-sight (NLOS) propagation, and the near-far problem due to non-zero cross-correlation between spreading codes. This last issue is the focus of this paper.

The near-far effect is very common in cellular wireless mobile communications systems. Its origin lies in the different attenuation losses incurred by the different propagation paths of the signals coming from different transmitters. Near-far is given when the receiver captures a strong signal, acquiring the wrong peak and making impossible the acquisition of weaker signals [4]. In GNSS, where the role of transmitters is played by the satellites, no near-far problems were supposed to show up since GNSS systems were initially designed to operate outdoors, in open-sky environments where the relative distances of the visible satellites to the Earth do not differ in orders of magnitude. However, when GNSS receivers are pushed to work in harsh environments, very different from those for which they were originally conceived, the near-far effect becomes detrimental due to the high attenuations incurred by the different materials that the signals from the satellites have to cross through.

The presence of near-far may lead to the following situations: 1) weak signals from satellites in view are not detected; 2) weak signals are detected but the pseudorange has a huge error; 3) a satellite not in view is declared to be present (false alarm). A first approach to prevent near-far from affecting the pseudorange computation consists in detecting its presence, and thus discarding the affected satellite, so that the user's position can be computed by using the rest of available satellites. This could be done in environments with great satellite availability. But in indoor environments, where the number of visible satellites for positioning is typically scarce, near-far mitigation techniques are therefore needed to re-enable the affected satellite.

In the literature, several solutions to mitigate near-far can be found. Linear multiuser detectors [5] have been shown to decrease interference effects in GPS receivers. However, they present high computational burden, and the noise may be enhanced throughout the mitigation process [6]. Alternatively, cancellation techniques [7] become attractive due to their low computational complexity and easy implementation. In this group, interference cancellation [8] (or soft near-far mitigation) techniques aim at identifying and subtracting the strong signals from the received input signal. This can be done by means of successive [9] or parallel [10] interference cancellation techniques (SIC and PIC, respectively), where signals are removed one by one or in blocks of many signals at each iteration. Nonetheless, their effectiveness is reduced when the parameters of interferences are not perfectly estimated, and

This work has been partially supported by the Spanish Ministry of Economy and Competitiveness project TEC2014-53656-R.

978-1-5090-2425-4/16/$31.00

furthermore, the presence of strong signal multipath and data-bit modulation can introduce additional interference [11].

Hard near-far mitigation techniques are also interference cancellation techniques, but subtraction is carried out by using algorithms based on projection operations. In this group, adaptive code replica techniques [12] consist in dispreading the received signal by using slightly modified versions of the original codes, which are more orthogonal to strong signals and may provide original codes with some immunity to interferences. This technique presents the advantage of taking into account time-varying working conditions. However, the reconstruction of codes in real time requires a significant amount of operations on vectors and matrices.

On the other hand, several studies have shown that subspace projection techniques are low-complexity hard near-far mitigation methods that outperform other techniques like successive cancellation. They are also less sensitive to errors in the synchronization parameters of interferences, and they produce small residual errors if such parameters are properly estimated. Moreover, recent sources have shown that they do not involve the estimation of the amplitudes and carrier phases of the interferences [13].

However, there are open challenges which are very relevant in practice but still have to be addressed. These refer to the analysis on how well subspace projection techniques perform against effects or processes that may have an impact in practice, in real handheld receivers. These include the robustness against synchronization errors of the strong signals, or errors in the detection of the data bits, or the effect of input signal filtering and quantization processes that take place at the front-end of real receivers. To the best of the authors' knowledge, some of these problems have been barely studied for GPS signals, but no efforts have been made for the future Galileo. The present paper is intended to bridge this gap by carrying out a detailed study on the sensitivity of projection-based near-far mitigation techniques against such effects. To do so, a simulation campaign is conducted using Galileo E1C signals for civilian use.

The rest of the paper is structured as follows. Section II presents the signal model and the basis of projection-based techniques, particularly the subspace projection technique, and a brief description of the algorithm. Section III quantifies the robustness of the technique in the presence of errors in the estimated synchronization parameters or data bits of the strong interferences. Section IV analyses how the performance of the technique is affected when the input signal is filtered or quantized at the receiver front-end. Section V draws the conclusions.

II. Preliminaries on near-far mitigation

A. Signal model

As a generic approach, the received signal is considered to be a contribution of L strong and M weak signals. The output signal at the receiver's front-end after down-conversion to baseband and sampling is shown in (1),

$$\mathbf{y} = \mathbf{S}\mathbf{a_s} + \mathbf{W}\mathbf{a_w} + \mathbf{r} \tag{1}$$

where $\mathbf{y} = \left[y\left(n_0\right), \ldots, y\left(n_{N-1}\right)\right]^T$ with N being the number of samples, $\mathbf{S} = \begin{pmatrix} s_1 & s_2 & \cdots & s_L \end{pmatrix}$ is an $N \times L$ matrix containing the strong signals in columns, with $\boldsymbol{s_i} = \left[s_i\left(n_0\right), \ldots, s_i\left(n_{N-1}\right)\right]^T$, and $\mathbf{W} = \begin{pmatrix} w_1 & w_2 & \cdots & w_M \end{pmatrix}$ is an $N \times M$ matrix containing the weak signals in columns, with $\boldsymbol{w_i} = \left[w_i\left(n_0\right), \ldots, w_i\left(n_{N-1}\right)\right]^T$. The strong $\boldsymbol{s_i}$ and weak $\boldsymbol{w_i}$ signals refer to unity amplitude samples of the down-converted signals, and thus $\mathbf{a_s} = \left[a_1, \ldots, a_L\right]^T$ is a vector containing the amplitudes of strong signals, and $\mathbf{a_w} = \left[a_{L+1}, \ldots, a_{L+M}\right]^T$ is a vector containing the amplitudes of weak signals. In (1), $\mathbf{r} = \left[r\left(n_0\right), \ldots, r\left(n_{N-1}\right)\right]^T$ is a vector containing additive white Gaussian (AWGN) noise.

B. Subspace projection technique

GNSS signals possess an inherent protection against near-far effects, which is provided by the use of spreading codes. However, in indoor applications, where signal attenuations can be up to 30 dB when propagating through concrete walls, such inherent protection is not enough to withstand near-far. It is limited to a certain upper bound, since the spreading codes used in GNSS are not completely orthogonal. For Galileo E1C, the protection for any non-zero Doppler shift is around 23 dB [14]. In this sense, the aim of near-far mitigation is to extend the protection against near-far up to the values of input near-far ratio (NFR) that can be reached in extreme situations in indoor environments (*i.e.* 35 dB) by means of signal processing techniques.

The conventional matched filter provides the optimal performance in scenarios affected by AWGN noise. When a weak signal is declared to be affected by near-far, there is the contribution of cross-correlation interference terms at the correlator output. Such contribution does not correspond to AWGN noise, and thus the traditional and standard matched filter fails to provide the optimum decision statistics. In this sense, projection-based techniques can be understood as some kind of matched filter designed for those cases where cross-correlation interferences do not correspond to white noise anymore but they are understood as some structured or colored noise.

The subspace projection technique is a particular method which treats the incoming signal as a contribution of strong signals and weak signals, which constitute the strong and weak signal subspaces, respectively. In the former, the parameters obtained from the acquisition of strong signals are used to form the subspace locally (*i.e.* local reconstruction of strong signals). Once all interferences are identified, the reconstructed subspace is then subtracted from the output signal at the receiver's front-end. In this way, we can remove the effect of disturbances from all the weaker signals simultaneously, allowing their acquisition afterwards [15].

The final objective of this technique is to remove the cross-correlation interference terms by using projection operations, so that the output signal is orthogonal to the subspace spanned by the interferences. According to figure 1, the signal of interest is the interference-free signal given by $\mathbf{P}_{\mathbf{P}_S^{\perp}\mathbf{H}}\mathbf{y}$. Then the standard matched filter can be used as usual with an interference-free input signal. It is also worth mentioning that this method is not restricted only to the near-far effect mitigation, but it can be used to reject any other similar type of interference in GNSS receivers [7].

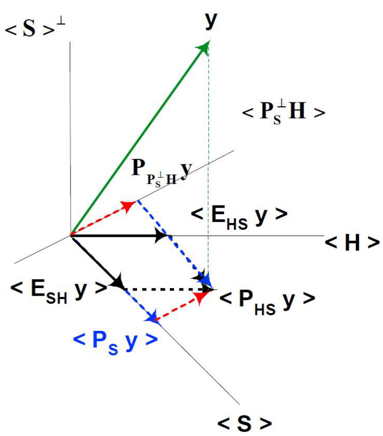

Fig. 1: Schematic representation of subspace projection method [7].

Let $y(n)$ be the samples of the output signal at the receiver's front-end. Let $\mathbf{S}$ be the generator matrix of the strong signal subspace of $y(n)$, and let $\mathbf{W}$ be the generator matrix of the weak signal subspace. The signal $y(n)$ can be expressed in matrix notation as shown previously in (1).

The projection operator in (2) needs to be used to compute the projection of the input signal onto the strong signal subspace, which represents the interference contribution, and gives (3),

$$\mathbf{P}_s = \mathbf{S}\left(\mathbf{S}^{H}\mathbf{S}\right)^{-1}\mathbf{S}^{\mathbf{H}} \tag{2}$$

$$\mathbf{P}_s\mathbf{y} = \mathbf{S}\mathbf{a}_\mathbf{s} + \mathbf{P}_s\mathbf{W}\mathbf{a}_\mathbf{w} + \mathbf{P}_s\mathbf{r} \tag{3}$$

where the component of weak signals can be neglected, since codes for weak signals are nearly orthogonal to each other [15], and their amplitudes are assumed to be much smaller than those for strong signals. This gives (4) as a result.

$$\mathbf{P}_s\mathbf{y} = \mathbf{S}\mathbf{a}_\mathbf{s} + \mathbf{P}_s\mathbf{r} \tag{4}$$

The portion of the input signal that lies on the interference subspace (*i.e.* the projected signal in (4)) is then subtracted from $y(n)$, giving as a result the interference-free signal in (5), which is orthogonal to the subspace spanned by interferences.

$$\mathbf{y}' = \mathbf{y} - \mathbf{P}_s\mathbf{y} = \mathbf{W}\mathbf{a}_\mathbf{w} + \mathbf{P}_s^{\perp}\mathbf{r} \tag{5}$$

III. Robustness of Subspace Projection Technique

In order to successfully apply the subspace projection technique, a local reconstruction of the strong interfering signal is needed. For this purpose, the synchronization parameters of such signal have to be estimated, namely the Doppler shift and code delay. To remove the interference completely, the estimated parameters have to match perfectly those from the real strong signal. But in practice, such parameters will contain errors with respect to the real values, and this will cause inherently distortion in the mitigation process. A portion of the interference will remain after mitigation (*i.e.* residual near-far effect). The impact of such estimation errors in the mitigation process has not been yet studied in the literature, and the robustness of subspace projection techniques against such errors of the strong signals still has to be confirmed.

In this sense, the distortion of the interference reconstruction d_R can be quantified as the residual portion of the interference after mitigation. Let $s(\tau)$ be the original strong signal, and let $\hat{s}(\tau)$ be the reconstructed version, with τ the time variable in samples. The distortion is computed as shown in (6) [3] and is unitless. In an ideal case where both signals are equivalent, distortion equals to zero.

$$d_R \doteq \frac{\sum_{k=0}^{N-1}|\hat{s}(\tau_k) - s(\tau_k)|^2}{\sum_{k=0}^{N-1}|s(\tau_k)|^2} \tag{6}$$

If the estimation errors are too large, the situation may lead to: 1) the weak desired signal cannot be acquired; 2) the weak signal is acquired but the pseudorange has a huge error. Thus, the aim of this section is to quantify the limits of subspace projection techniques before they lose their effectiveness due to the presence of such estimation errors, that is, the maximum estimation errors that they can stand. The techniques are considered to lose their effectiveness when the NFR after mitigation exceeds the inherent protection of spreading codes. For this analysis, simulations are carried out considering one weak signal which is affected by near-far by one strong signal, which simulates a harsh scenario with very reduced satellite availability.

A. *Robustness against Doppler shift errors*

In high-sensitivity GNSS receivers (*i.e.* C/N_0 of 15 dB-Hz), the Doppler frequency error of locally reconstructed interferences should not surpass 0.2 Hz to allow acquiring the weak signal [15]. On the other hand, it is worth mentioning that a large value of input NFR represents a strong interference, but it is desirable in the extent that the Doppler shift can be estimated reliably. However, although a lower value

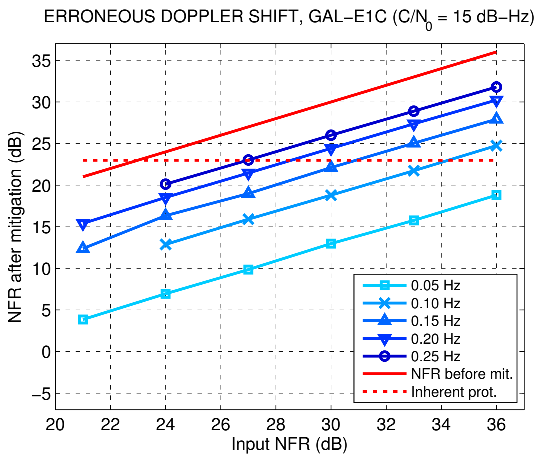

Fig. 2: Mean NFR after mitigation versus input NFR for C/N_0 of 15 dB-Hz, analysis of how the technique is affected by errors in the estimated interfering Doppler shift.

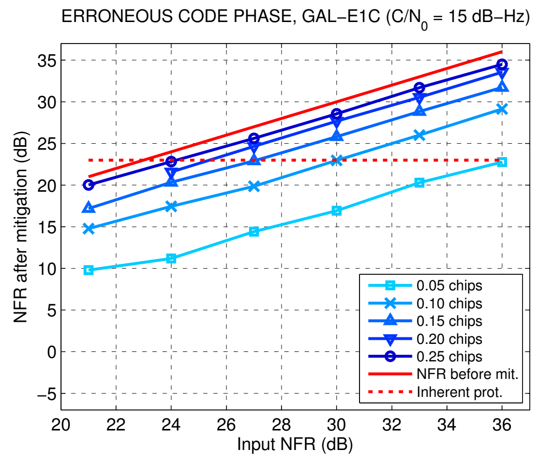

Fig. 3: Mean NFR after mitigation versus NFR for C/N_0 of 15 dB-Hz, analysis of how the technique is affected by errors in the estimated interfering code delay.

of input NFR represents a weaker interference, it may pose difficulties in obtaining accurate Doppler shift estimates since the interference may not be strong enough for this purpose.

For these reasons, simulations are carried out for a perfect estimation of the code delay but errors in the estimated Doppler shift ranging from 0.05 Hz, which simulates the former case, to 0.25 Hz, which simulates the latter case. Figure 2 shows the simulation results in terms of mean residual NFR after mitigation versus input NFR. The maximum NFR that the technique can tolerate refers to that value of input NFR for which the resulting NFR after mitigation equals to the inherent protection of spreading codes, which is considered to be 23 dB as stated previously.

As expected, the presence of Doppler shift errors has an impact on the performance of mitigation, since the maximum input NFR that the technique can tolerate tends to decrease as errors increase. It is for an error of 0.10 Hz that the technique is limited to an input NFR up to 35 dB. The technique provides an additional protection over spreading codes ranging from 11 dB to down to 4 dB for the considered errors, which remains constant for all values of input NFR (*i.e.* the slope of NFR after mitigation is constant for all values of input NFR). The distortion, which is computed as shown previously in expression (6), also increases along with errors, ranging from 0.1290 to 2, which reveals that indeed Doppler frequency errors in the reconstructed signal cause a portion of the interference to remain after mitigation.

B. *Robustness against code phase errors*

Following the same fashion as in Section III-A, simulations are now carried out for a perfect estimation of the Doppler shift but errors in the estimated code delay, ranging from 0.05 chips to 0.25 chips to cover the range of input NFR up to 35dB. These values recreate scenarios from high to low input NFR, respectively, in the sense that high NFR is desirable to accurately estimate the interferent code delay with small error, and low values NFR lead to higher errors when estimating such parameter.

Figure 3 shows the simulation results in terms of mean residual NFR after mitigation versus input NFR. In the best case, mitigation provides an additional protection over spreading codes of 13 dB or more in the presence of errors up to 0.05 chips. On the other hand, mitigation provides almost no improvement over spreading codes for errors exceeding 0.20 chips. The additional protection keeps constant regardless of the input NFR. In view of these results, errors in the estimated code delay of interferences should not exceed 0.10 chips, so that mitigation can handle values of input NFR above 30 dB in indoor scenarios. Distortion ranges in this case from 0.3 to 1.5, and similarly to Section III-A, this concludes that a portion of the interference remains after mitigation in the presence of code delay errors.

C. *Errors in the data bits*

In the likely case where the strong interfering signal has not only pilot but also data channel, the latter must also be locally reconstructed to mitigate near-far when subspace projection techniques are used. The applicability of the technique may be compromised when bit transitions are not correctly identified. This occurs when the strong signal is a data component but it is not strong enough in absolute terms to reliably estimate the data, and the coherent integration period exceeds the duration of a bit [11]. This is applicable to high-sensitivity GNSS receivers, where the coherent correlation time usually exceeds the duration of a bit to deal with low values of C/N_0. The value of the data bits also needs to be estimated, so that the data channel of the reconstructed version matches the one from the actual interference comprised in the input signal. If not correctly estimated, the presence of powerful misidentified data bits in the projected signal may also contribute to near-

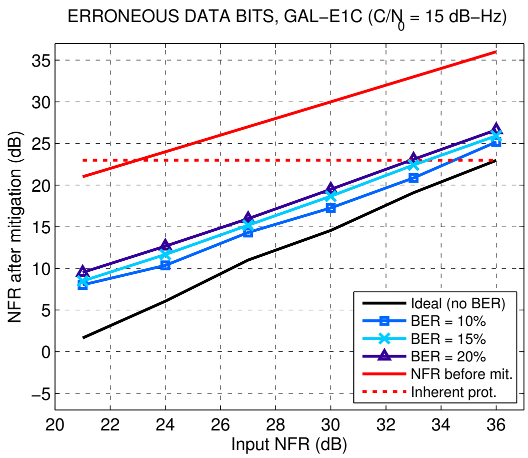

Fig. 4: Mean NFR after mitigation versus input NFR for C/N_0 of 15 dB-Hz, analysis of how the technique is affected by errors in the estimated interfering data bits.

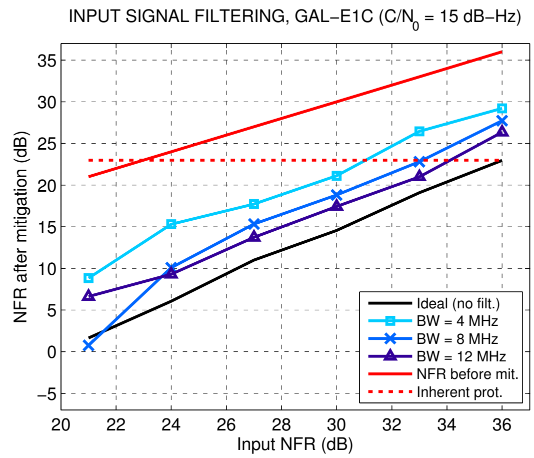

Fig. 5: Mean NFR after mitigation versus input NFR for C/N_0 of 15 dB-Hz, impact of input signal filtering on near-far mitigation.

far due to non-zero cross-correlation, and similarly to sections III-A and III-B, a portion of the strong signal may remain in the projected signal after mitigation.

However, in the particular case of Galileo E1C, misidentification of data bits is expected to have a minor impact on mitigation, since pilot signals are used and cross-correlation may affect only the data component. In order to prove this, simulations are carried out for extremely large values of bit error rate (BER), namely 10%, 15% and 20%. As stated, the simulation results in figure 4 show small performance deterioration with respect to the case with zero BER, in which case the subspace projection technique can tolerate an input NFR of 36 dB. For BER as large as 15% or 20% the performance is lost for input NFR of 33 dB, representing a difference of only 3 dB with respect to zero BER.

This is in contrast with the fact that distortions range from 0.6296 to 0.8476 from best to worst BER, thus making evident the presence of residual near-far after mitigation. In spite of this, the small performance deterioration observed in figure 4 proves the claim in [13] that the use of data-less pilot signals for acquisition in Galileo E1C reduces considerably the impact of this problem.

IV. Sensitivity to front-end signal conditioning

Subspace projection techniques are known to be good performers of near-far mitigation. Nevertheless, several open questions still remain open to make the technique usable in practice. The objective of this section is to determine the sensitivity and performance of subspace projection techniques when the incoming signal is conditioned by the receiver's front-end, namely input signal filtering and quantization.

A. *Input signal filtering*

One of the most important aspects that is always overlooked in the studies about near-far mitigation is that the front-end of a GNSS receiver always includes a filtering step of the incoming signal, whereas the projection operation assumes that the signal is unfiltered. This translates into a modified waveform of the real subspace containing the interferences, with respect to the reconstructed version. This gives rise to a mismatch between the actual subspace containing the strong signals and the subspace used in the projector, and similarly to Section III, this causes a portion of the interference to remain after mitigation. This also reduces the near-far interference that can be handled by the mitigation method.

For BOC codes (such as Galileo E1C), the minimum filter bandwidth is twice the sum of chipping rate and offset code rate [16]. Thus, the minimum practical bandwidth for Galileo E1C is 8 MHz. From this standard value, filters with smaller bandwidth (*i.e.* 4 MHz) may be used for low-accuracy but low-cost receivers, whereas filters with bandwidth up to 16 MHz are used in receivers that are required to provide enhanced accuracy.

For these reasons, simulations are carried out for filter bandwidths of 4 MHz, 8 MHz and 12 MHz. The simulation results in figure 5 show that indeed the additional protection decreases as the filter bandwidth becomes narrower. In the best case, for a bandwidth of 12 MHz, the technique experiments a loss of additional protection of 2 dB with respect to the ideal case without filtering. In the worst case, the loss increases to 5 dB.

According to the numbers in figure 5, the technique provides an additional protection over spreading codes that ranges from 11 dB to 8 dB, involving that the maximum values of input NFR that the technique can tolerate range from 34 dB to 31 dB. Similarly to the results in Section III, such additional protection remains constant for all possible values of input NFR.

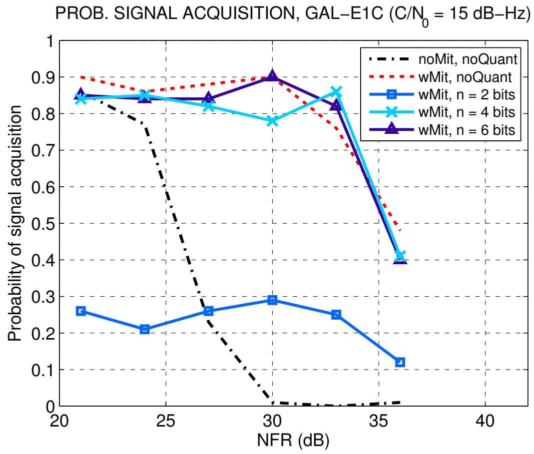

Fig. 6: Probability of signal acquisition after mitigation when input signal is quantized, for C/N_0 of 15 dB-Hz.

B. Signal quantization

Similarly to Section IV-A, the front-end of a GNSS receiver also includes a quantization step of the incoming signal with as few bits as possible so as not to increase complexity. On the other hand, the projection operation usually increases the required number of quantization levels of the signal after mitigation. According to [8], in order to properly represent the clean mitigated signal, the required number of quantization bits ranges from 7 to 12 bits for input NFR values ranging from 21 to 36 dB. Thus, a requantization of the mitigated signal using a similar number of levels as in the incoming signal is needed also for the sake of complexity.

However, whereas input signal sampling is done in the receiver's front-end at hardware level, the subsequent signal processing is carried out at software level, since software receivers are being considered. This means that mitigation can be carried out using a large number of bits without compromising the receiver's complexity. This assumption is in line with the spread of software-defined solutions, where both stages are decoupled, and it is not necessary to keep the same number of bits in the operation in both phases.

Nevertheless, the requirements of the hardware front-end are more restrictive. In order to keep the hardware complexity of the front-end low, commercial receivers are often equipped with A/D converters of 2 quantization bits, or even as few as 1 quantization bit in the case of mass-market receivers. In order to see what the impact of quantizing the incoming signal with such low number of bits would be, simulations are carried out for 2, 4 and 6 quantization bits. The simulation results reveal no major deterioration of the performance of the subspace projection technique.

However, even in software-defined architectures, quantization causes the probability of signal acquisition to drop (*i.e.* probability of signal detection), see figure 6. The reason for this is that, when quantizing the input signal, the actual C/N_0 decreases depending on the number of bits used. The most relevant case is given for 2 bit quantization, since it involves the major loss of C/N_0, namely 0.55 dB [17]. As a consequence of a lower C/N_0, the integration time in the acquisition stage may become insufficient for reliably detecting signals. Thus, quantizing the input signal may cause the integration time to be increased in the receiver's acquisition stage. On the other hand, 4 bit and 6 bit quantization produces negligible degradation, in comparison to the ideal case without quantization.

V. Conclusions

This paper has focused on the subspace projection technique for near-far mitigation purposes in high-sensitivity GNSS receivers. However, the main contribution of the paper is the analysis of the sensitivity and quantization of the performance limits of the technique against different concerns that cause a negative impact on the mitigation process. To the best of the authors' knowledge, the impact of these effects has not been studied in the literature, but constitutes a fundamental step towards making the subspace projection method applicable in real handheld receivers such as smartphones.

On one hand, the robustness against errors in the estimated synchronization parameters and data bits of strong signals has been studied. In the latter, the results have shown that cross-correlation has no major effect when acquiring the pilot signal. On the other hand, the hardware front-end of GNSS receivers includes input signal filtering and quantization steps, and simulation results have revealed that the former has an impact on the performance of mitigation, whereas the latter produces a drop rather in the probability of signal acquisition after mitigation caused by a loss of C/N_0.

The maximum input NFR tolerated by the technique has been determined for all cases. Simulation results have shown that the portion of interference that remains after mitigation increases as the aforementioned situations become more extreme, involving a decrement of the additional protection over spreading codes provided by projection-based mitigation techniques.

Further work to be done includes analysing these effects considering multiple weak and strong signals, and corroborate the results with real data measurements.

References

[1] G. Lopez-Risueno and G. Seco-Granados, "Detection and Mitigation of Cross-Correlation Interference in High-Sensitivity GNSS Receivers," in *Personal, Indoor and Mobile Radio Communications, 2007. PIMRC 2007. IEEE 18th International Symposium on*, Sept 2007, pp. 1–5.

[2] ——, "CN0 estimation and near-far mitigation for GNSS indoor receivers," in *Vehicular Technology Conference, 2005. VTC 2005-Spring. 2005 IEEE 61st*, vol. 4, May 2005, pp. 2624–2628.

[3] F. Sousa and F. Nunes, "Near-far effect mitigation for GNSS software receivers using subspace projection," in *Satellite Navigation Technologies and European Workshop on GNSS Signals and Signal Processing (NAVITEC), 2010 5th ESA Workshop on*, Dec 2010, pp. 1–6.

[4] T. S. Rappaport, *Wireless Communications: Principles And Practice, 2nd Edition*.

[5] S. Verdú, *Multiuser Detection*. Cambridge University Press, 1998.

[6] B. Lu, J. Zhong, M. Zhao, and L. Li, "A near-far effect canceller for GPS high sensitivity receiver," in *Position Location and Navigation Symposium (PLANS), 2012 IEEE/ION*, April 2012, pp. 341–346.

[7] E. P. Glennon and A. G. Dempster, "A Review of GPS Cross-Correlation Mitigation Techniques," *The 2004 International Symposium on GNSS/GPS*, 2004.

[8] L. chen, W. Meng, S. Han, and E. Liu, "A Cross-Correlation Mitigation Method Based on Subspace Projection for GPS Receiver," *Proceedings of the 25th International Technical Meeting of The Satellite Division of the Institute of Navigation (ION GNSS 2012)*, pp. 1428–1434, September 2012.

[9] P. Madhani, P. Axelrad, K. Krumvieda, and J. Thomas, "Application of successive interference cancellation to the GPS pseudolite near-far problem," *Aerospace and Electronic Systems, IEEE Transactions on*, vol. 39, no. 2, pp. 481–488, April 2003.

[10] E. P. Glennon, R. C. Bryant, A. G. Dempster, and P. J. Mumford, "Post Correlation CWI and Cross Correlation Mitigation Using Delayed PIC," *Proceedings of the 20th International Technical Meeting of the Satellite Division of The Institute of Navigation (ION GNSS 2007)*, pp. 236–245, September 2007.

[11] E. P. Glennon and A. G. Dempster, "A Novel GPS Cross Correlation Mitigation Technique," *Proceedings of the 18th International Technical Meeting of the Satellite Division of The Institute of Navigation (ION GNSS 2005)*, pp. 190–199, September 2005.

[12] C. Lacatus, D. Akopian, and M. Shadaram, "An Adaptive Approach to Compensate Cross-Correlation Effects in Weak Signal Conditions for Satellite Positioning Systems," Fort Worth, TX, September 2007, pp. 990–998.

[13] F. Nunes and F. Sousa, "GNSS Near-Far Mitigation through Subspace Projection without Phase Information," *Aerospace and Electronic Systems, IEEE Transactions on*, vol. 48, no. 3, pp. 2746–2755, JULY 2012.

[14] S. Locubiche-Serra, J. A. López-Salcedo, and G. Seco-Granados, "Statistical Near-Far Detection Techniques for GNSS Snapshot Receivers," *International Conference on Acoustics, Speech and Signal Processing (ICASSP)*, Mar 23 2016.

[15] Y. Morton, J. Tsui, D. Lin, L. Liou, M. Miller, Q. Zhou, M. French, and J. Schamus, "Assessment and Handling of CA Code Self-Interference During Weak GPS Signal Acquisition," *Proceedings of the 16th International Technical Meeting of the Satellite Division of The Institute of Navigation (ION GPS/GNSS 2003)*, pp. 646–653, September 2003.

[16] K. Borre, D. Akos, N. Bertelsen, P. Rinder, and S. Jensen, *A Software-Defined GPS and Galileo Receiver: A Single-Frequency Approach*, ser. Applied and Numerical Harmonic Analysis. Birkhäuser Boston, 2007.

[17] D. Borio, "A Statistical Theory for GNSS Signal Acquisition," Tesi di Dottorato, Politecnico di Torino, 2008.